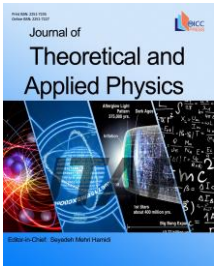

J. Theor. Appl. Phys., 2026; 20(3): 255-262

Journal of Theoretical and Applied Physics (JTAP)

https://doi.org/10.57647/jtap.2026.2018.0308

Research Article

Plasmonic Random Laser Based on Deformed Double Metallic Core Shell NPs

Saddam Faliheh Haddawi*[1], Elaf A. Kadhem[1], Fatemeh Gholami[2]

[1]*Department of Laser Physics, College of Science for Woman, University of Babylon, Babylon, Iraq*
[2]*Magneto-plasmonic Lab, Laser and Plasma Research Institute, University of Shahid Beheshti, Tehran, Iran*

***Corresponding author:** Shaddawi@yahoo.com

Article History:

Received:
25 January 2026

Revised:
16 February 2026

Accepted:
24 February 2026

Published Online:
05 March 2026

Published in Issue:
30 June 2026

Abstract

In this study, the production and characterization of silver, core-shell gold-silver and core-shell silver-gold nanoparticles, as well as the effect of a random laser with Rhodamine 6G gain medium by applying an external voltage, were investigated. These plasmonic nanoparticles were produced by laser ablation in liquid and pumped with 532 nm nanosecond pulse laser. By increasing the pumping energy above the threshold, the fluorescence spectrum of the plasmonic nanoparticle is amplified. Based on the results, narrow peaks emerged with a full width at half maximum less than 10 nm, with the number of spikes increased with FWHM about (0.42 and 0.34 nm) for Ag@Au NPs and Ag*@Au NSs, which is suitable for the manufacturing of compact and miniaturized random laser sources.

Keywords: Random laser, Plasmonic nanoparticles, Core-shell, External voltage

Cite this article: Haddawi, S.F., kadhem, E.A., Gholami, F., (2026). Plasmonic Random Laser Based on Deformed Double Metallic Core Shell NPs. *J. Theor. Appl. Phys.*, 20(3), 255-262. https://doi.org/10.57647/jtap.2026.2018.0308

1. Introduction

A random laser is an optical device that requires a gain medium and cavity to provide a feedback mechanism. Dye solutions are used as the gain medium, and multiple scattering also plays the role of cavities. Multiple scattering increases the photon's residence time in the medium, amplifies the light, and increases the intensity of the laser beam [1]. Depending on the type of this feedback, random lasers can be divided into two types: (1) random lasers with incoherent feedback (2) random lasers with coherent feedback [2]. In incoherent random lasers, when a particle is scattered, it will change the direction of propagation. In this type of laser, the path of light is open, which means that the scattered photon doesn't return to its original scattering position and escapes from the random medium [3]. Strong scattering in the active medium plays an important role in incoherent feedback. Multiple scattering increases the path length and then returns to the original point and forms a closed-loop so that the photons are trapped in a random environment and the amplification of the light occurs by the stimulated diffusion process. Laser spikes in the emission spectrum are the main features of this type of random laser [4, 5]. Different configurations of random lasers have been investigated so far, such as Dye solutions with dispersed nanoparticles [6], dye-polymer

films with embedded nanoparticles [7], dye-doped nematic liquid crystals [8], a photonic crystal fiber inserted with a dye solution and nanoparticles [9]. Metal nanoparticles can be used to improve the performance of random lasers [10-11]. Metal nanoparticles have significant scattering cross-sections that can effectively scatter light. These nanoparticles also have surface plasmon resonance (SPR), which can confine light close to the surface, activate the high gain for lasing and increase the light locally through SPR. The scattering of metal nanoparticles can be controlled by the type of nanoparticles, shape and particle size. Among metal nanoparticles, gold and silver nanoparticles have received much attention due to the absorption of surface plasmon (SPR) in the visible region and increasing the field amplitude [12, 13]. One of the effective methods to achieve coherent random laser and broadband scatterer is the use of core-shell nanoparticles [14, 15]. In this study, we produced gold NPs, silver NPs, Au@Ag, and Ag@Au core-shell NPs and in a new shape (Au*@Ag, and Ag*@Au core-shell NPs) by laser ablation in liquid (LAL) method as scattering points in the gain media. We used the Rhodamine 6G (Rh6G) as a gain medium. The effect of external voltage on the deformation of nanoparticles and the increase in energy on their radiation spectrum on the performance of the random laser will be studied.

2. Experimental methods

In this report, we used different nanoparticles as our random laser scattering centers, which include: gold NPs, silver NPs, Au@Ag, and Ag@Au core-shell NPs. laser ablation method in the liquid used to produce spherical nanoparticles and their new shape by applying external voltage in 5 directions of the cell containing the target. When an external voltage is applied, the nucleus of an atom senses a force equal to the direction of the external electric field equal to Eq. A negatively charged electron cloud feels the same amount of force, but in the opposite direction to the electric field. As a result of the external force, the nucleus moves in the direction of the electric field until the external force applied to it is canceled by the force applied to the nucleus by the electron cloud [14]. This external voltage changes the shape of the sample from spherical to star (Au*@Ag, and Ag*@Au core-shell NSs). We used the first harmonic generation of the Q-switched Nd: YAG laser with a repetition rate of 10 Hz and a pulse width of 4 nanoseconds with an energy of 66 mJ. Then a lens with a focal length of 15 cm and a mirror with an angle of 45 degrees was used to focus the laser beam as shown in Figure (1). To investigate the effect of a random laser, the nanoparticles were combined with Rh6G dye solution and sonicated for 10 minutes. The dye solution was prepared in ethanol having a concentration of 10^{-5} M. after that prepared gain medium done by mixing (2 ml) from a fixed dye concentration Rh6G (1.5x10-5 M) with (1 ml) from each the noble metal samples, and the fabricated samples were stirred at room temperature (RT) in an ultrasonic bath for about 20 min to obtain the best homogeneity for these samples. Finally, for random laser action, it was used the second harmonic generation of the Q-switched Nd: YAG laser was (532 nm, 4 ns, 10 Hz). The reflected radiation at an angle of 45 degrees is transmitted to the spectrometer (Avantes) by optical fiber and from the spectrometer is connected to the computer with the interface wire as shown in Figure (2).

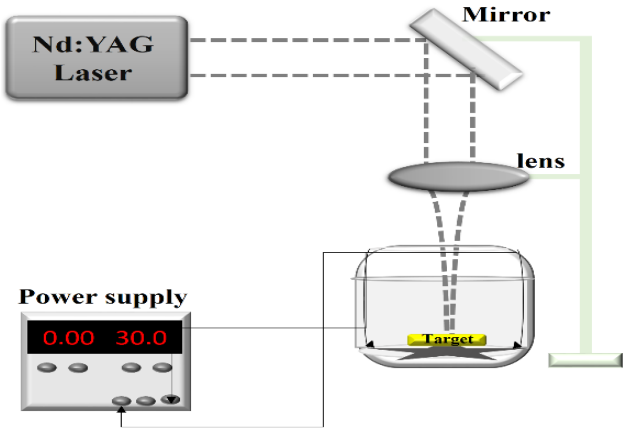

Figure 1. Schematic of the experimental setup of laser ablation method

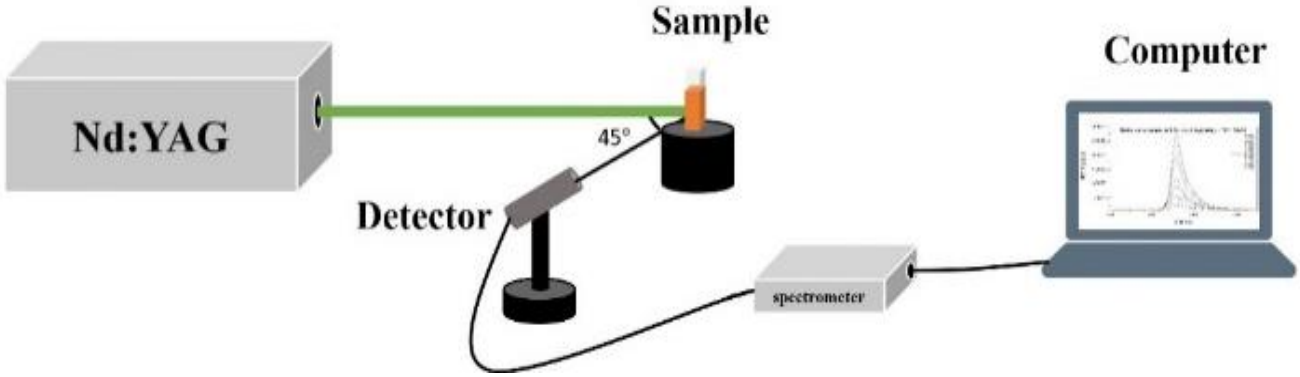

Figure 2. Schematic of the experimental setup of the random laser system

10.57647/jtap.2026.2018.0308

3. Results and discussions

3.1. Characterization of nanoparticles

Figure (3.a) represents the images of the Ag nanostar which was prepared by the laser ablation technique in deionized water as a host medium.

Colloidal Ag nanostar has been generated with sizes approximately (50 nm) which was checked by transmission electron microscopy (TEM), and the sizes were determined by image program, Ag*@Au and Au*@Ag core-shell nanostar have been used as scattering centers in a random medium containing Rh6G as the gain medium with average particle size for the core diameter (50 nm) and (10 nm) for the shell thickness as shown in Figure (3. b and c) respectively. The absorption spectrum of Au, Au *, Ag, and Ag * nanoparticles are shown in Figure 4-a. The absorption peaks of both Ag and Au nanoparticles are reduced after an external voltage is applied, and the peak SPR intensities of Au nanoparticles towards the longer wavelengths (red shift) from 526 nm for Au NPs to 538 nm for Au * at, and 402 nm for Ag NPs to 410 nm for Ag *NSs. The absorption spectrum of Ag@Au, Ag*@Au, Au@Ag, and Au*@Ag nanoparticles are shown in Figure (4.b) the black curve represents the absorption of Ag@Au core-shell NPs of the core size 50 nm and shell thickness 10 nm has a peak at 405 nm, while the red line indicates to the absorption peak of Ag*@Au core-shell NSs decreases with the redshift at the same size which has a peak at 413 nm, and for each of them observed the small peak SPR of Au shell thickness. The blue and green lines in the Figure (4.b) are the absorption peak of Au@Ag core-shell NPs and Au*@Ag core-shell NSs, respectively, also decreases with the redshift from 531 nm to 538 nm, and the peak SPR intensity of Ag NPs is not visible and the Au NPs effect is predominant. The absorption spectrum of Rh6G is shown in Figure 5 The best absorption spectrum of Rh6G was obtained at concentration 1 *10-5 M at 531 nm, and good overlap between the resonant wavelength and the Rh6G wavelength is the ideal way to achieve a low-threshold plasmon-based random laser, so this concentration will be adopted for random laser action.

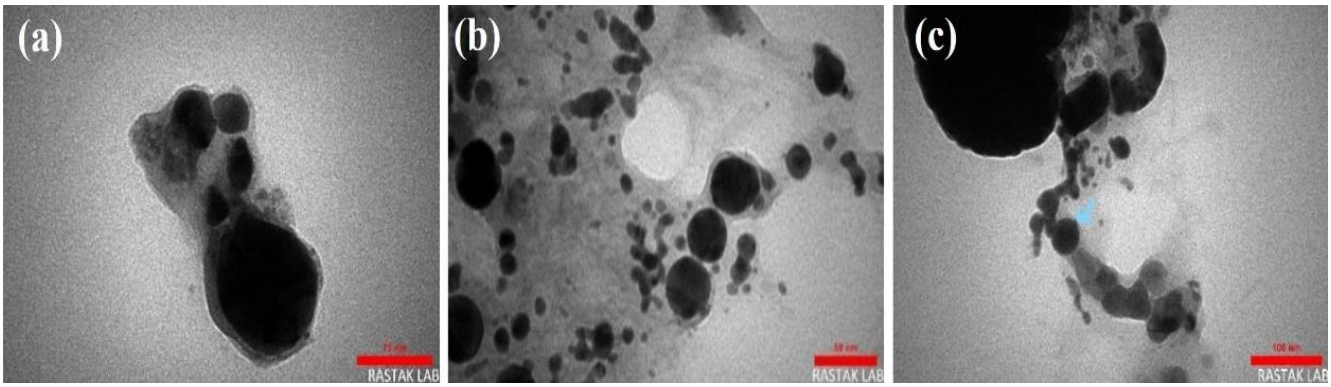

Figure 3. Shows TEM images of a) Ag*, b) Ag*@Au and c) Au*@Ag produced by laser ablation method with an external voltage

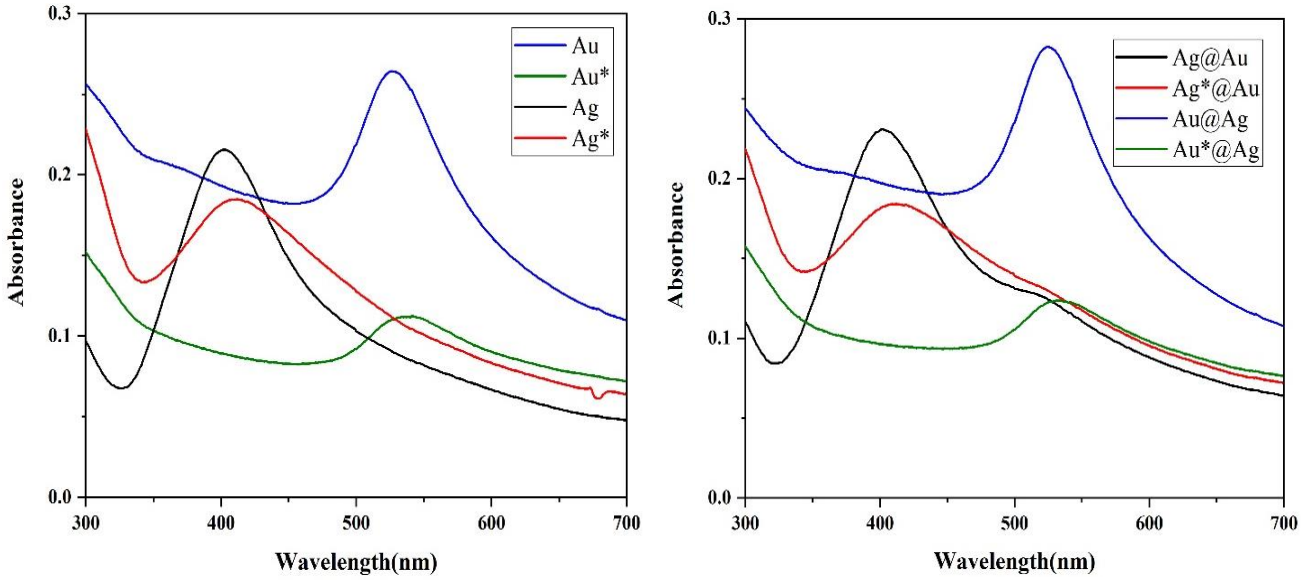

Figure 4. Absorbtion spectrum of a) Au, Au*, Ag and Ag* b) Ag@Au, Ag*@Au, Au@Ag and Au*@Ag

10.57647/jtap.2026.2018.0308

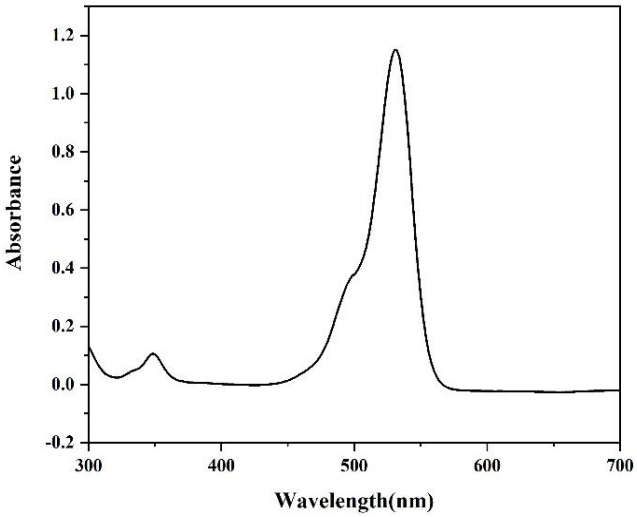

Figure 5. Absorbtion spectrum of Rhodamin 6G

3.2. Random laser

In this section, we used Rh6G dye with concentration of 10^{-5} M dispersed in ethanol with six different types of nanoparticles (Ag, Ag*, Ag@Au, Ag*@Au, Au@Ag, and Au*@Ag) as the gain medium. The random laser properties of these samples pumped by 532 nm have been investigated. As shown in the Figure (6. a-f) the scattering centers of these media demonstrate enough optical feedback, and the influence of the pumping energies on the emission spectra of these samples was prominent. For all samples at the lowest pumping energy 24 μJ, It is noticed that there is incoherent random laser emission appears, and gradually, as the energy of the laser pump increases, the number of photons in the sample increases, and allow to photons travel a long way and then return to the main point and form a closed loop, so the photons are trapped in a random environment, and multiple scattering occurs more frequently.

In this case, reach to coherent random laser the peak emission spectrum has several discrete spikes that appear to reach less than 1 nm with the intensity increased.

The Figures (6. a and b) show the random laser characteristics, and the data were collected in the Ag NPs and Ag* NSs samples. for Ag NPs At low pumping energies at 24 μJ, broad emission spectrum with a peak at 556 nm, by increasing in the pump energy above the threshold in the Ag NPs, the emission spectra of the random laser become narrow together with an increase of the peak intensity to (23596 a.u.) with FWHM (13nm), also the spikes more clear and increase in number and this means the possibility of the emergence of the coherent random laser as shown in Figure (6. a). Where it was found from the Figure (6. b) that the emission intensity for Ag*NSs reaches (24259.33 a.u.) and the value of FWHM (11.7 nm) with enhance in the number of spike with FWHM less than 0.85 nm, due to an increase in the optical path in the Ag*NSs and confinement of emitted light by multiple scattering, Which results from the sharp edges of the surface of this sample.

Thus the value of scattering mean free path (l_s) will be reduced by changing the shape of NPs from (4.6 to 4.3 mm) for Ag NPs or Ag*NSs, respectively, and this parameters of mean free path for each sample had been calculated by the relation: $l_s = \frac{T}{\ln\frac{I_0}{I}}$ in each type of NPs by the cell thickness, T, the transmitted intensity of the solvent, I_0 and the transmitted intensity of the solvent with Ag NPs or Ag*NSs, I.

The Figure (6. c and d) study new kind of gain medium contain different shape core-shell with fixed thickness (Au@Ag NPs and Au*@Ag NSs) mixed with fixed concentration of Rh6G (10-5 M), so by this style, can enhance random laser emission with reduce threshold gain and FWHM. Where the analysis of results has been shown a quite different in the random laser properties with change samples type.

Figure (6. c and d) gives the emission spectrum results of the random laser system for Au@Ag NPs and Au*@Ag NSs). after the pumping energy increase above the threshold, observed that the emission spectrum for Au*@Ag NSs compared with Au@Ag NPs results where the emission peak increases from (18503 a.u. to 21124 a.u.), and the FWHM decreases from 10.9 nm to 10 nm and number of spike increased with FWHM less than (0.78 and 0.65 nm) respectively. as shown results, where it has been observed that the value of (ls) decrease by changing the shape of the core-shell NPs, and this behavior is more pronounced Au*@Ag NSs used as a scattering center, and the value of (l_s) reaches to (3.8 mm), while the value in the Au@Ag NPs reach to (4 mm). This result is attributed to much large scattering cross section in the Au*@Ag NSs sample.

again to improving the properties of the random laser by changing the shell of the scattering centers, the Figure (6. e and f) shows a different evolution in the emission spectra of the Au and Au* shell active media than that of the previous media which had been illustrated in Figures (6. a-d), The threshold gain could be reduced remarkably when the change of shell type and its shape.

This will reduce the amount of light energy lost in the shell. So observed in these samples the value of the emission spectrum will be enhanced (19127 and 30890 a.u.) for Ag@Au NPs and Ag*@Au NSs, also the FWHM more narrowed in the FWHM reach to (9.3 and 8.5 nm), the number of spikes increased with FWHM about (0.42 and 0.34 nm), and observed that the value of the (l_s) is reduced by the Au and Au* shell sample to (3.4 and 2.9 mm), respectively.

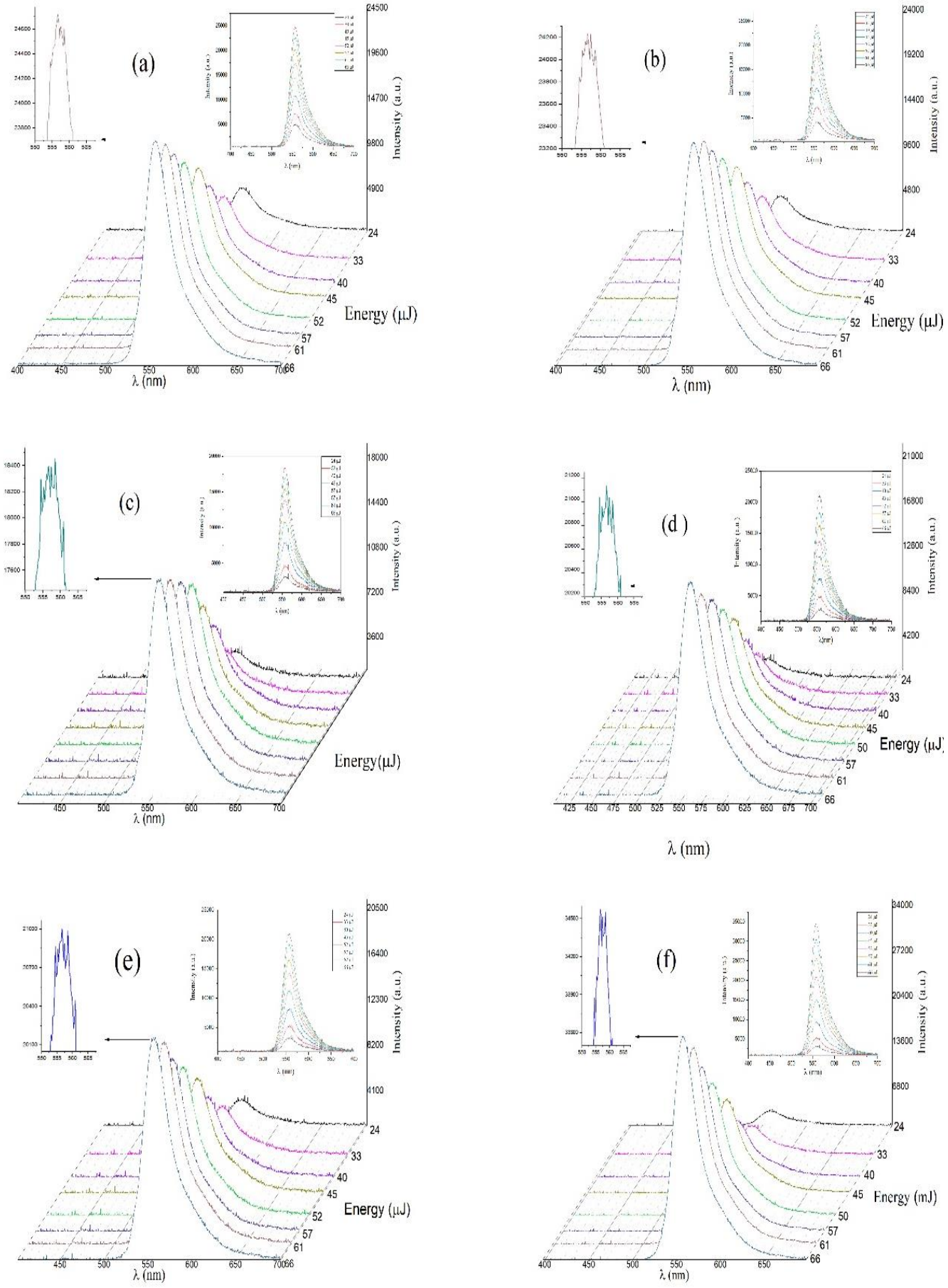

Figure 6. Emission spectra of (a) Ag NPs and (b) Ag* NSs(c) Au@Ag NPs and (d) Au*@Ag NSs (e) Ag@Au NPs and (f) Ag*@Au NSs

10.57647/jtap.2026.2018.0308

as it was observed that spikes emergence was related to where after the pumping energy above the threshold, in Figure (7. a) shows how the number of spikes has evolved by changing the shape and type the shell of the samples. It has been noted that their number of spikes with Ag@Au NPs sample is more than that in Au@Ag NPs samples, and also with higher intensity peak, due to investigate the effected of local field enhancement on lasing resonance in Au NPs shell. So the time of the stay of the photon inside the random medium will be longer with higher interactions and thus the possibility of amplifying it and obtaining a coherent laser output increases, and the same behavior goes back to the Ag@Au NPs and Ag@Au* NSs samples as shown in the Figure (7. b). In Figure 8 It is obvious that the threshold gain of Au*@Ag NSs is lower than that of Ag*@Au NSs because of its much larger scattering cross-section of it. The lowest pump threshold occurred near the edge of the diffusive regime, corresponding to a scattering mean free path. Now we examined the output laser of six different samples at the same pump energy (66 μJ), in the Figure (9) shows how the number of spikes has evolved by changing the shell from Ag to Au, and observed the best result in the sample Ag*@Au NSs.

As we mentioned in a previous section that Au shell have a much larger scattered cross section than that of the Ag NPs at the same dimensional (Figure 10).

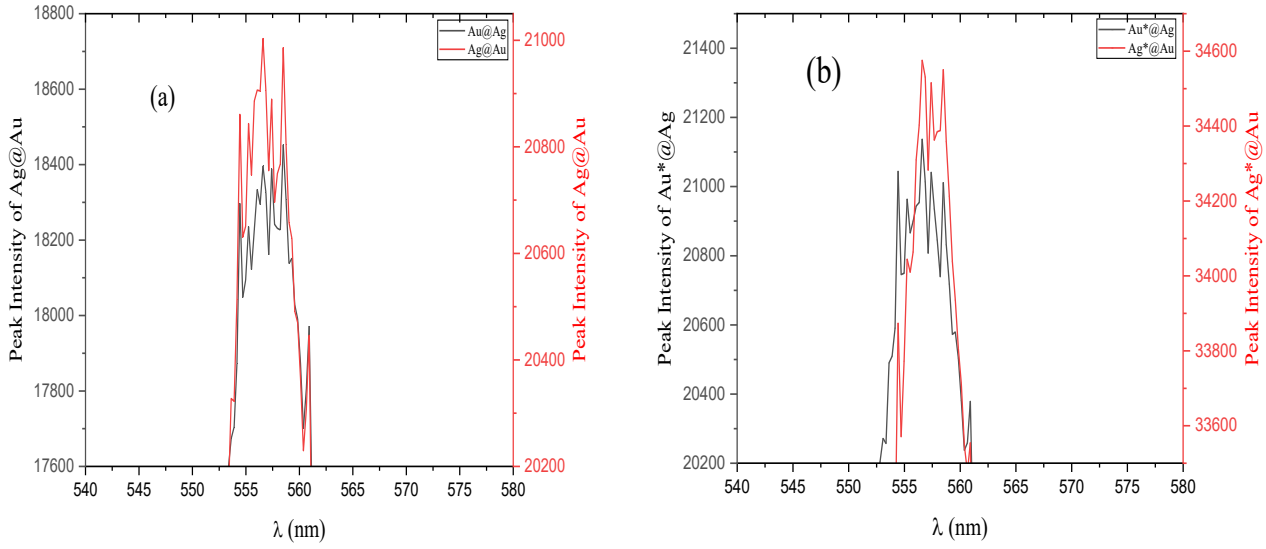

Figure 7. Comparison of the radiation spectrum intensity of core-shell nanoparticles a) spherical b) with an external voltage

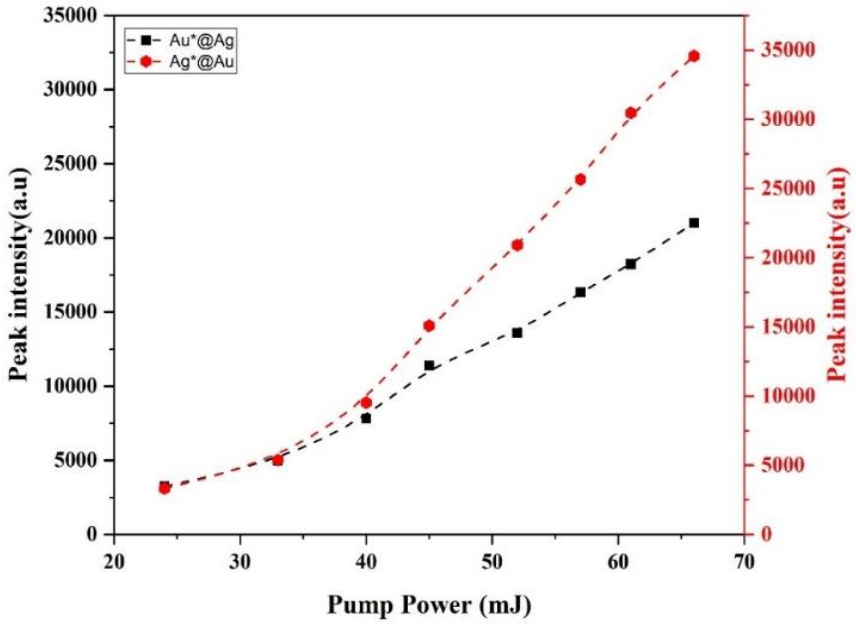

Figure 8. Comparison of the radiation threshold intensity spectra of core-shell nanoparticles with an external voltage

10.57647/jtap.2026.2018.0308

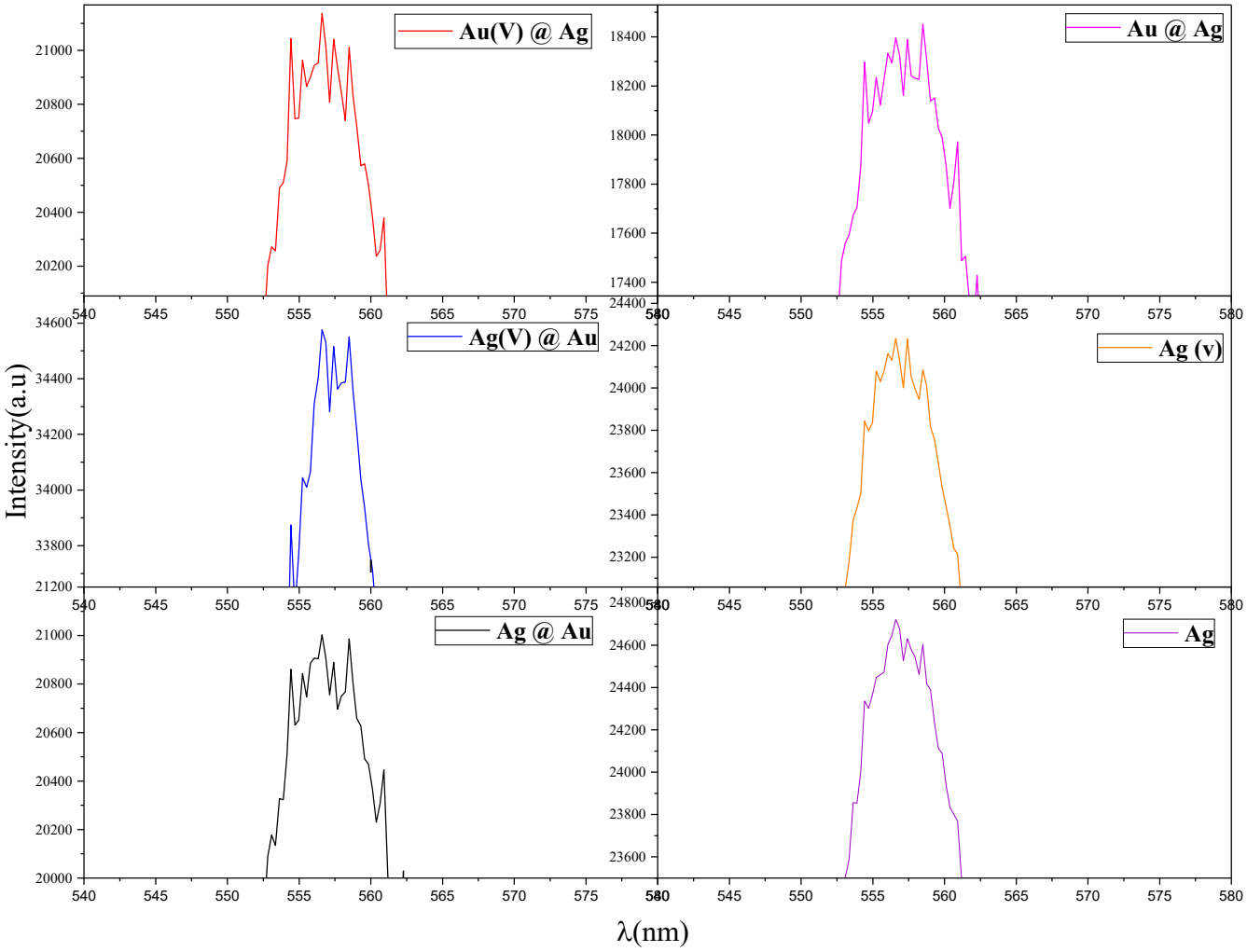

Figure 9. Radiation spectra of nanoparticles at a maximum energy of 66 mJ

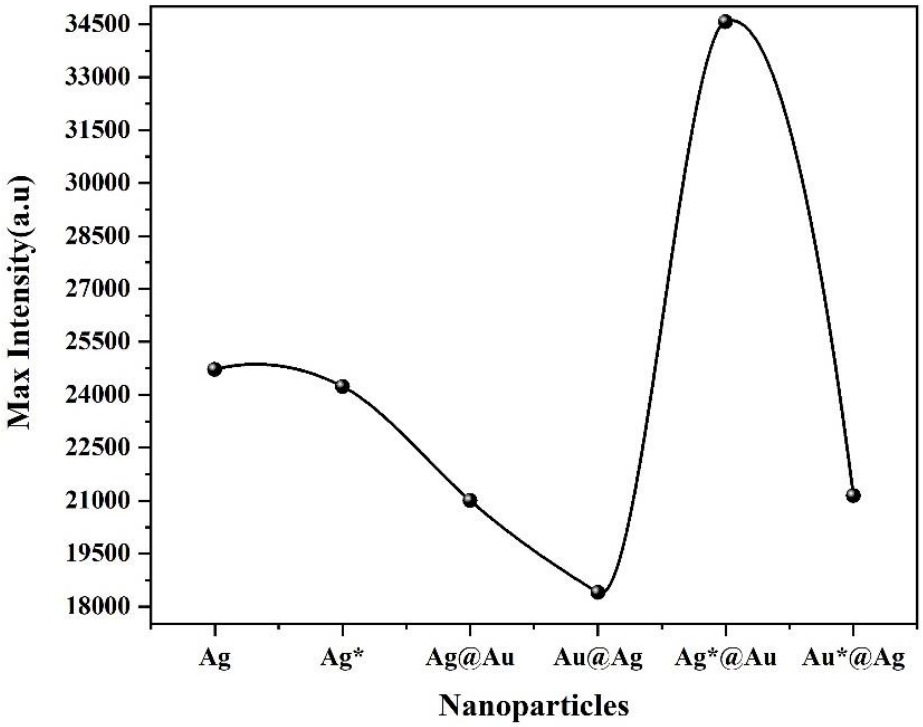

Figure 10. Maximum radiation spectrum intensity according to the type of nanoparticles

10.57647/jtap.2026.2018.0308

4. Conclusion

In thid report, we produce plasmonic nanoparticles (Ag, Ag*, Ag@Au, Ag*@Au, Au@Ag and Au*@Ag) by laser ablation method. We investigated the random laser properties of these nanoparticles mixed with Rh6G dye (10^{-5} M) as the gain medium by pumping a 532 nm nanosecond pulse laser. According to the radiation spectrum intensity diagrams, it was observed that by increasing the laser pumping energy from 24-66 μJ, the number of photons in the sample increases, and more scattering occurs more often, and the intensity of the radiation spectrum increases. In addition to increasing the laser pumping energy, applying voltage also improves the performance of random lasers in the core-shell nanoparticles by increasing the number of electrons and changing the sample size. Comparing the intensity threshold of the radiation spectrum of Ag *@Au and Au*@ Ag samples, we found that Ag*@ Au sample with threshold energy of 33 μJ has the highest intensity and best random laser performance.

Authors Contribution
All the authors have participated sufficiently in the intellectualcontent, conception and design of this work or the analysis andinterpretation of the data (when applicable), as well as the writingof the manuscript.

Availability of data and materials
The data that support the findings of this study are available fromthe corresponding author, upon reasonable request.

Conflict of interests
The authors declare that they have no known competing financialinterests or personal relationships that could have appeared toinfluence the work reported in this paper.

References

[1] Y. Nastishin and T. H. Dudok, “Optically pumped mirrorless lasing. A review. part I. random lasing,” Ukr. J. Phys. Opt., vol. 14, no. 3, pp. 146–170, 2013.

[2] S. F. Haddawi, N. Roostaei, and S. M. Hamidi, “Coupled modes enhance random lasing in plasmonic double grating structure,” *Optics & Laser Technology*, vol. 156, p. 108577, 2022.

[3] Feng Luan, Bobo Gu, Anderson S.L. Gomes, Ken-Tye Yong, Shuangchun Wen, Paras N. Prasad, “Lasing in nanocomposite random media”, Nano Today, vol.10, pp.168- 192, Apr. 2015.

[4] H. Cao, J. Y. Xu, S. H. Chang, and S. T. Ho, “Transition from amplified spontaneous emission to laser action in strongly scattering media,” Phys. Rev. E - Stat. Physics, Plasmas, Fluids, Relat. Interdiscip. Top., vol. 61, no. 2, pp. 1985–1989, 2000.

[5] A. Tulek and Z. V. Vardeny, “Studies of random laser action in π-conjugated polymers,” J. Opt. A Pure Appl. Opt., vol. 12, no. 2, 2010.

[6] S. F. Haddawi, H. R. Humud, Sakineh Almasi Monfared, and S. M. Hamidi, “Two-dimensional plasmonic multilayer as an efficient tool for low power random lasing applications,” *Waves in Random and Complex Media*, vol. 34, no. 3, pp. 1640–1649, Jun. 2021

[7] Polson, Randy C., Arkadi Chipouline, and Z. Valy Vardeny. "Random lasing in π-conjugated films and infiltrated opals." *Advanced Materials* 13.10 (2001): 760-764.

[8] Strangi, G., et al. "Random lasing and weak localization of light in dye-doped nematic liquid crystals." *Optics Express* 14.17 (2006): 7737-7744.

[9] de Matos, Christiano JS, et al. "Random fiber laser." *Physical review letters* 99.15 (2007): 153903.

[10] D.S.Wiersma, A. Lagendijk, Phys. Rev. E 54 (1996) 4256—4265**.**

[11] Johnson, Peter B., and R-WJPrB Christy. "Optical constants of the noble metals." *Phys. Rev. B* 6, no. 12 (1972): 4370.

[12] Philip, Reji, Panit Chantharasupawong, Huifeng Qian, Rongchao Jin, and Jayan Thomas. "Evolution of nonlinear optical properties: from gold atomic clusters to plasmonic nanocrystals." *Nano letters* 12, no. **9** (2012): 4661-4667.

[13] S. F. Haddawi, A. R. Sadrolhosseini, R. A. Ejbarah, S. M. Hamidi, and M. Kazemzad, “Chitosan-C3N4-Plasmonic Nanocomposite as a Generation of Scatterer Points for Random Laser Application,” *Plasmonics*, vol. 20, no. 9, pp. 7183–7193, 2025.

[14] Roostaei, N., et al. "Red and Blue color production by flexible all-dielectric structure." *Optik*, vol. 230, 2021, p. 166345.

[15] Jawad, Mariam K., et al. "Temperature dependent random laser performance of Au@Cu and Cu@Au core-shell nanoparticles in a rhodamine 6G–PNIPAM smart polymer matrix medium." *Optik*, vol. 338, 2025, p. 172499.